Supplementary Information

A novel kilogram-scale preparation method of $Na_{3.5}V_{1.5}Mn_{0.5}(PO_4)_3$ cathode material with excellent performance for sodium-ion pouch cells

Xin Tang [a,c,1], Jinhan Teng [a,c,1], Kaibo Zhang [a,c], Binghan Dai [a], Tianming Lu [a], Junjie Huang [a], Enmin Li [a], Weifeng Deng [b], Juncheng Zhou [d], Xing Wang [e, *], Jing Li [a,b, *]

[a] State Key Laboratory of Environment-friendly Energy Materials, School of Material Science and Engineering, Southwest University of Science and Technology, Mianyang 621010, Sichuan, China

[b] Engineering Research Center of Biomass Materials (Ministry of Education), School of Materials and Chemistry, Southwest University of Science and Technology, Mianyang, 621010, Sichuan, China.

[c] Sichuan Qing Yan Super Energy Capacitor Technology Co., Ltd., Suining 629201, Sichuan, China

[d] School of Mechatronics Engineering, Chengdu University of Technology, Chengdu 610051, Sichuan, China

[e] School of Materials Science, Northwestern Polytechnical University, Xi'an 710072, Shanxi, China

* E-mail: stellarwangwx@163.com (Xing Wang)

xy13787103391@126.com (Jing Li)

Section S1 Calculation process of sodium ion diffusion coefficient (D_{Na}^{+}):

The D_{Na}^{+} can be calculated using the following equation:

$$D_{Na}^{+} = \frac{4}{\pi\tau}\left(\frac{m_B V_M}{M_B S}\right)^2\left(\frac{\Delta E_s}{\Delta E_t}\right)^2 \quad (1)$$

in which τ is the intermittent time, m_B means the mass of the active substance, M_B represents the molecular weight of the active substance, V_M means the molar volume of the positive electrode material, ΔE_s is the difference of circuit voltage after 60min, and ΔE_t is the voltage difference within a time period τ (10 min) at 0.1 C.

Section S2 Calculation process of D_{Na}^{+} based on impedance fitting:

Base on the electrochemical impedance spectroscopy (EIS) results, the high frequency region of the Nyquist curve is semi-circular, which represents the charge transfer impedance (R_{ct}) between the electrode material and the electrolyte interface. The low-frequency region presents a straight line, which is related to the Walburg impedance (Z_w) of Na^+ diffusion in the electrode material.

The calculation equation of D_{Na}^{+} is as follows:

$$Z' = R_e + R_{ct} + \sigma\omega^{-1/2}$$

$$D_{Na^+} = \frac{R^2T^2}{2A^2n^4F^4C^2\sigma^2}$$

In the formula, R、T、A、n、F、C、σ represent the gas constant, the Kelvin temperature at room temperature, the electrode material area (diameter of 14 mm), the number of electrons transferred in the reaction, the Faraday constant, the Na^+ bulk concentration, and the Warburg impedance factor (the slope of the curve), respectively.

Section S3 Preparation method of sodium-ion full-cells:

To improve the energy density of full-cells, the cathode ingredient was adjusted to NVMP/PVDF/SP/Ketjen Black = 93.5:3:3:0.5, and the anode ingredient was adjusted to HC/CMC/SBR/SP = 94:2.5:2.5:1. The surface density (double-sided) of cathode and anode electrodes are 2.4 and 1.25 g dm^{-1}. Aluminum foil is used as the current collector for both cathode and anode electrodes. And aluminum and nickel were respectively used as the positive and negative electrode lugs.

The anode and cathode electrodes were assembled into the cells with each design capacity of 8.5 Ah by the lamination process, and then the cells were encapsulated by aluminum-plastic film. $NaPF_6$ (1 M) in EC/DEC/FEC = (6:3.5:0.5 vol %) was used as the electrolyte. The amount of electrolyte injection is controlled between 8.5 and 9 g/Ah. After high-temperature aging (50 ℃ for 48 h), formation, second sealing and capacity grading, the sodium-ion batteries can be tested and used.

Section S4 Preparation method of lithium-ion full-cells:

The commonly used cathode materials for lithium-ion batteries include ternary layered cathode ($LiNixCoyMnzO_2$, x+y+z = 1) and $LiFePO_4$, of which $LiFePO_4$ has good cycling performance. In order to comprehensively compare with sodium-ion batteries, both $LiNi_{0.8}Co_{0.1}Mn_{0.1}O_2$ and $LiFePO_4$ are prepared as lithium-ion pouch full-cells with each design discharge capacity of 8.5 Ah. Aluminum foil and copper foil are respectively used as the cathode and anode current collector. $LiPF_6$ (1 M) in EC/DEC/FEC = (6:3.5:0.5 vol %) was used as the electrolyte. Graphite is used as the anode material. Due to the significantly lower adsorption rate of graphite anode on electrolyte compared to HC anode, the amount of electrolyte injection is controlled to 3.5 g/Ah.

In addition to the above differences, the other preparation processes of lithium-ion batteries (such as cathode and anode ingredients, surface density, high-temperature aging, formation, etc.) are completely the same as those of sodium-ion batteries. The lithium-ion batteries containing $LiNi_{0.8}Co_{0.1}Mn_{0.1}O_2$ cathode are used for safety performance testing (such as the needle puncture, thermal shock and short-circuit testing, etc.), while the lithium-ion batteries containing $LiFePO_4$ are used for rate, low-temperature and cycling testing.

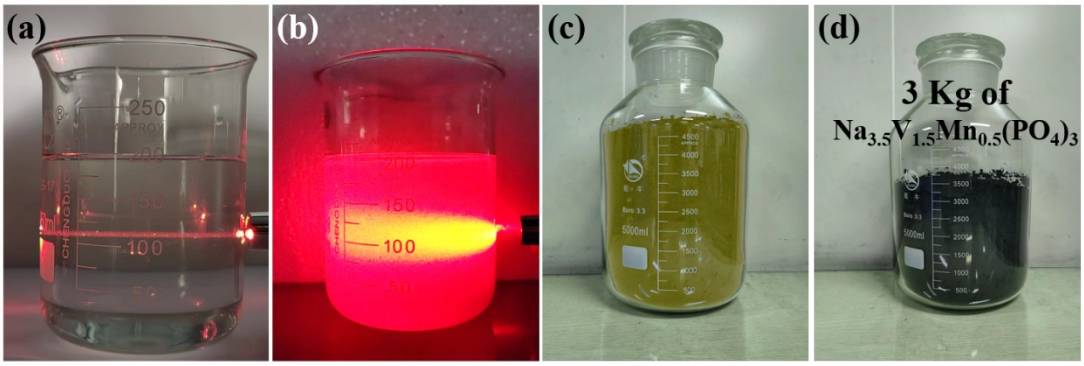

Figure S1. The Tyndall effect of (a) CMC colloid and (b) after mixing with Starch Solutions, and physical pictures of (c) precursor and (d) final product.

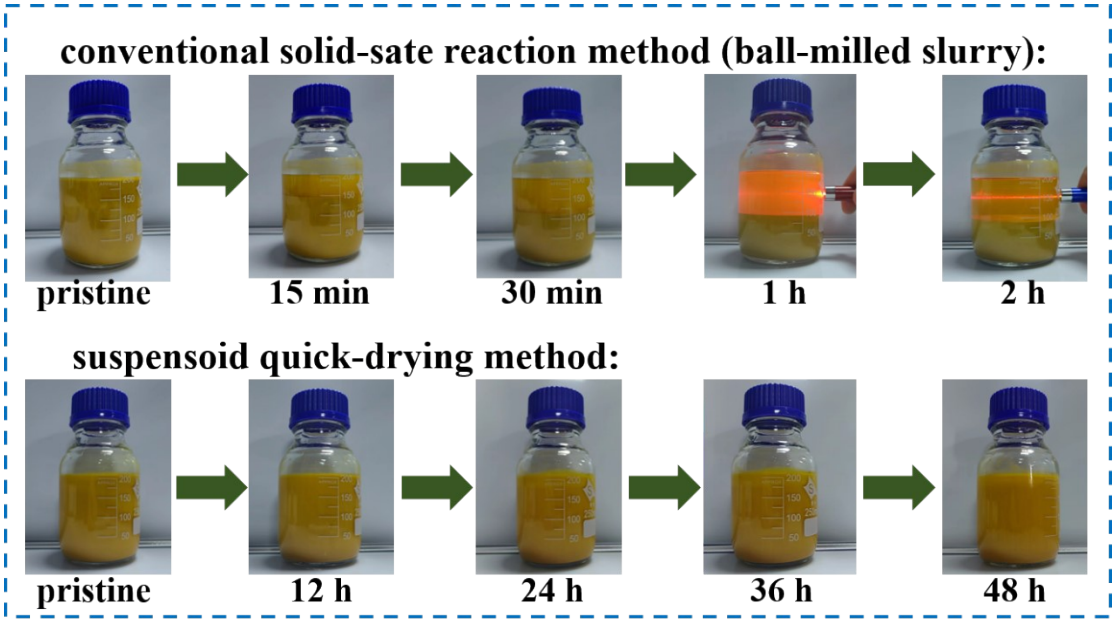

Figure S2. The Tyndall effect of (a) CMC colloid and (b) after mixing with Starch Solutions, and physical pictures of (c) precursor and (d) final product.

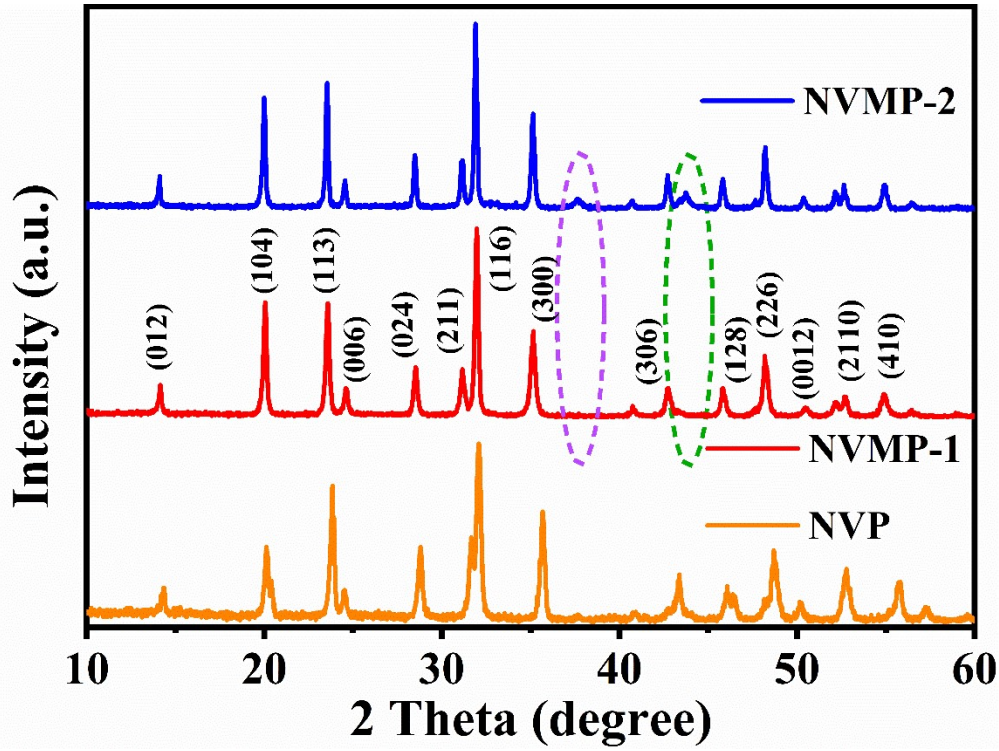

Figure S3. XRD patterns of NVMP-1, NVMP -2 and NVP.

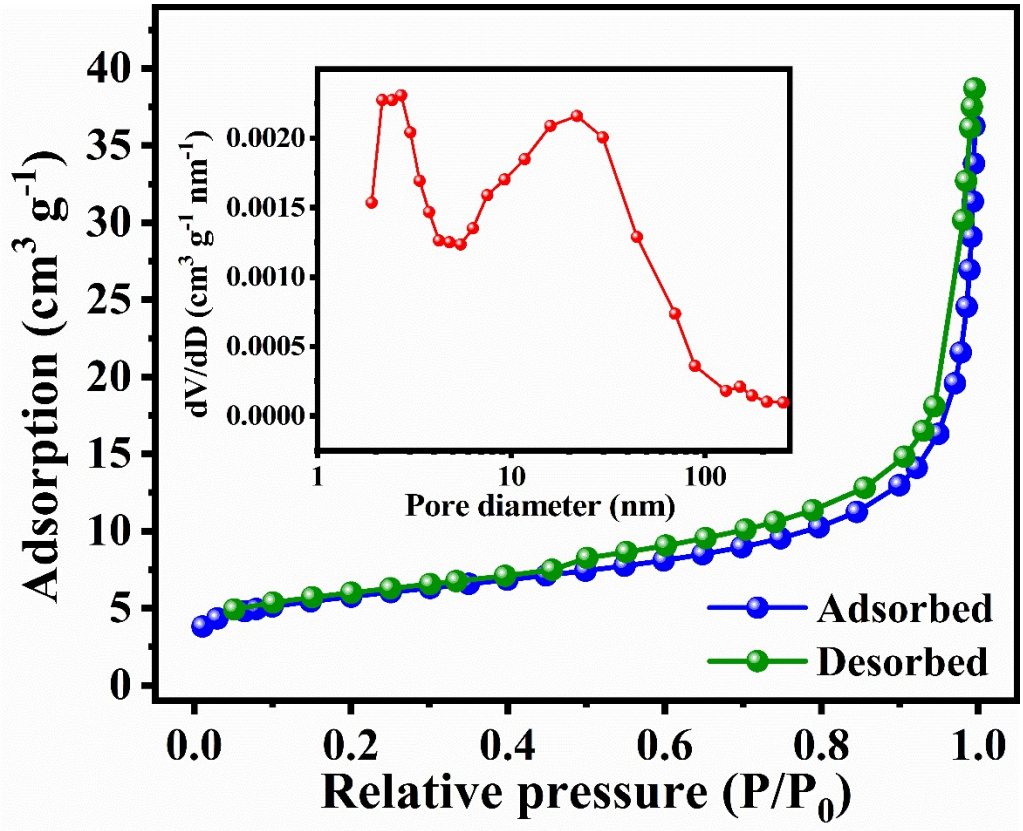

Figure S4. The nitrogen adsorption–desorption curve and pore-size distribution of NVMP-2.

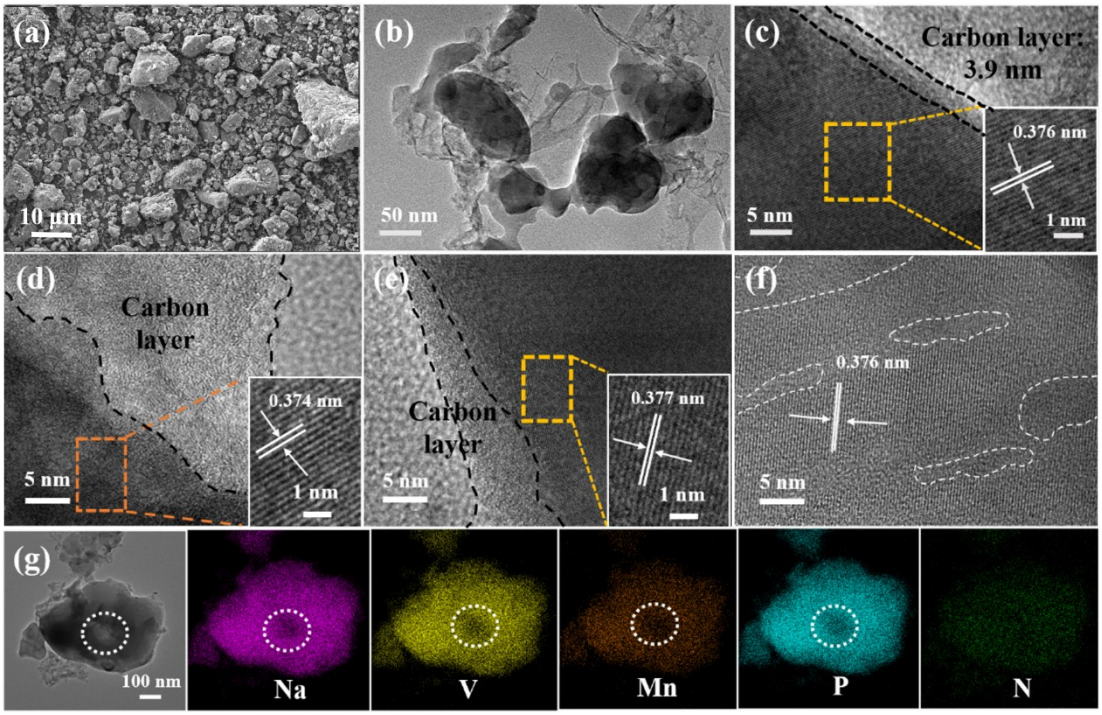

Figure S5. Microtopography images of NVMP-2: **(a)** SEM image, (**b**) TEM images, (**c-f**) HRTEM image and **(g)** EDS element mapping images of NVMP-2.

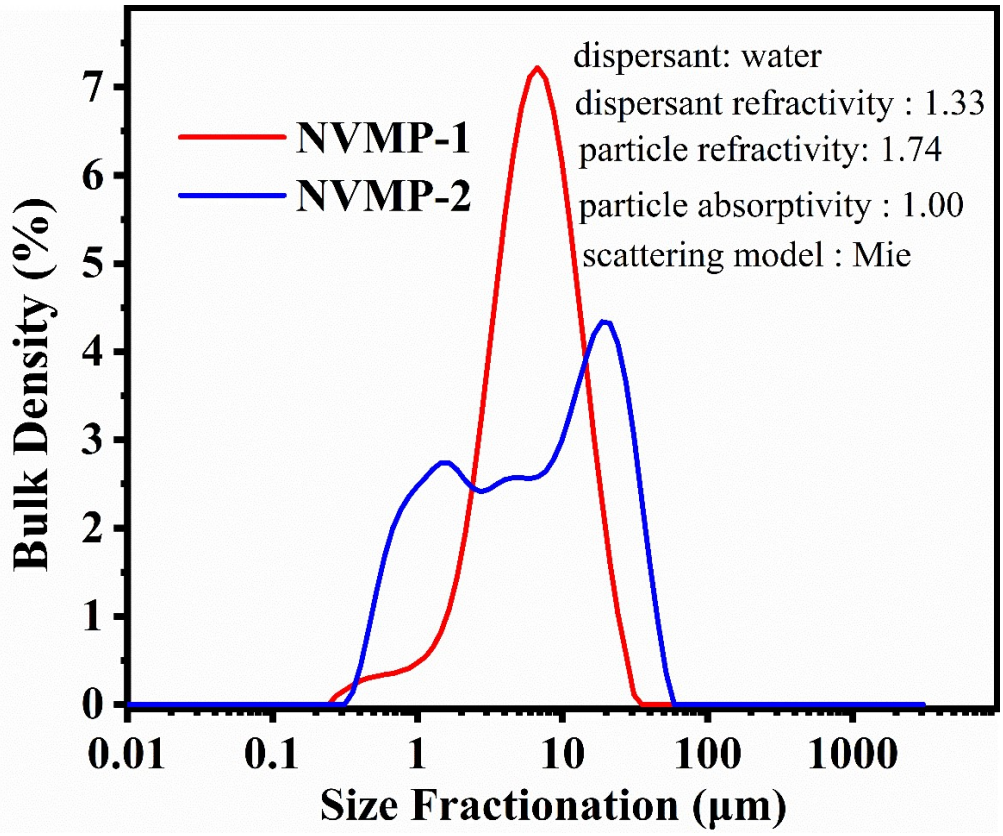

Figure S6. The particle size distribution curves of NVMP-1 and NVMP -2.

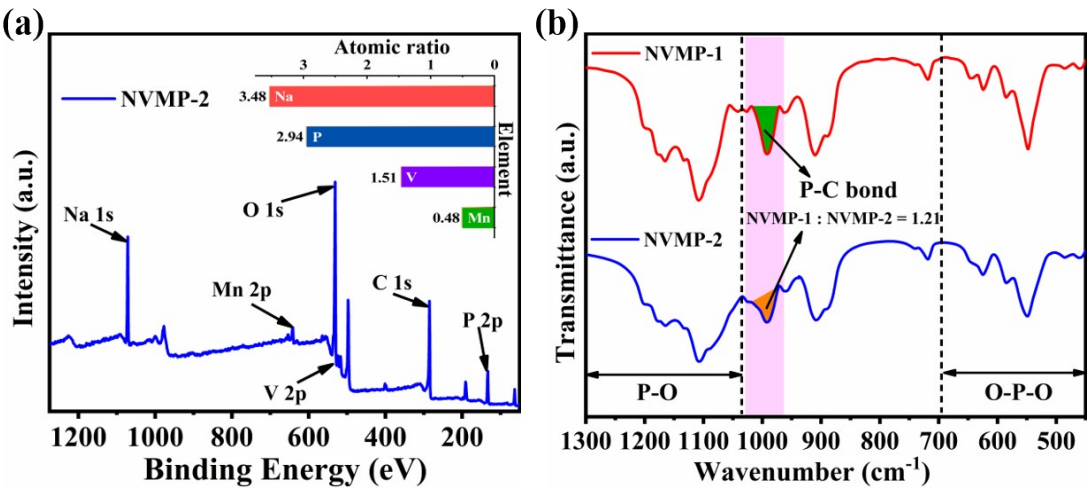

Figure S7. (a) XPS spectra in wide-range scanning and ICP result (inset) of NVMP-2, (b) FTIR spectrums of NVMP-1 and NVMP-2.

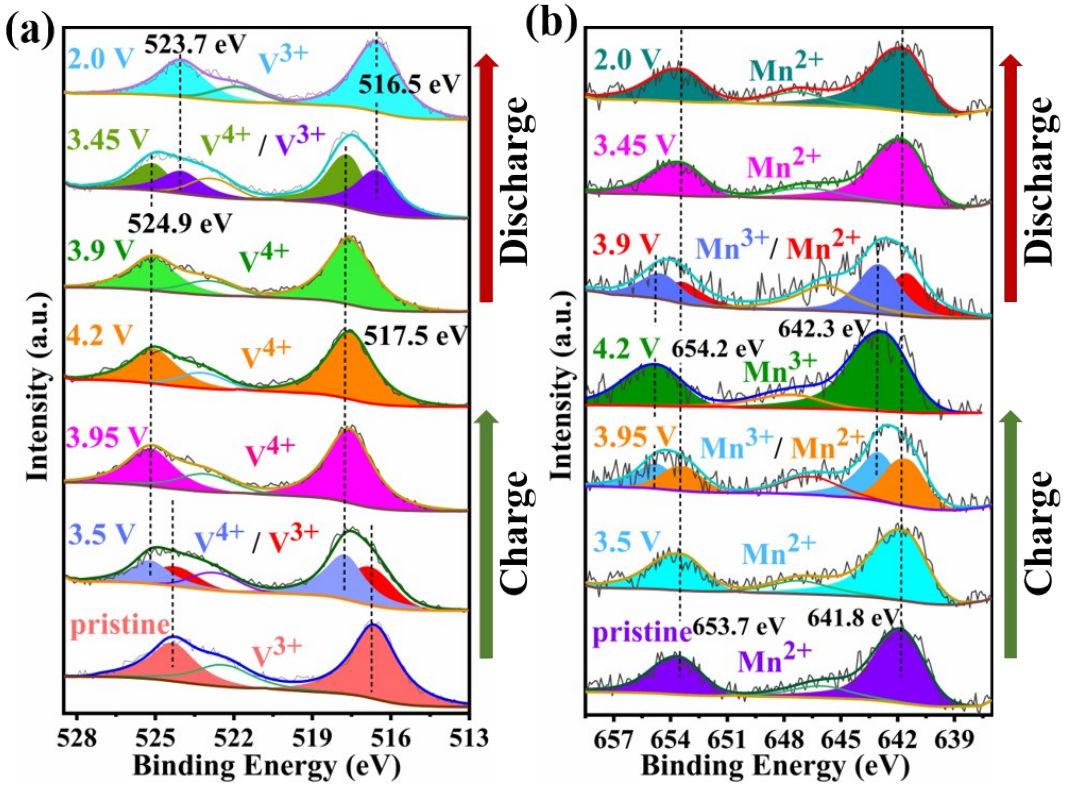

Figure S8. Ex-situ XPS spectra for (a) V 2p, (b) Mn 2p of NVMP-1 at different potentials in initial charge/discharge process.

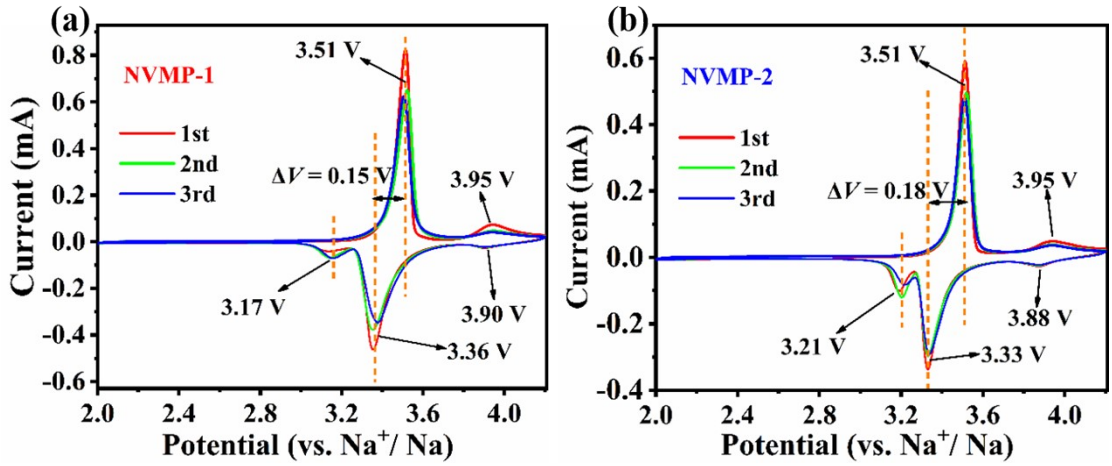

Figure S9. The comparison of CV curves of NVMP-1 and NVMP-2.

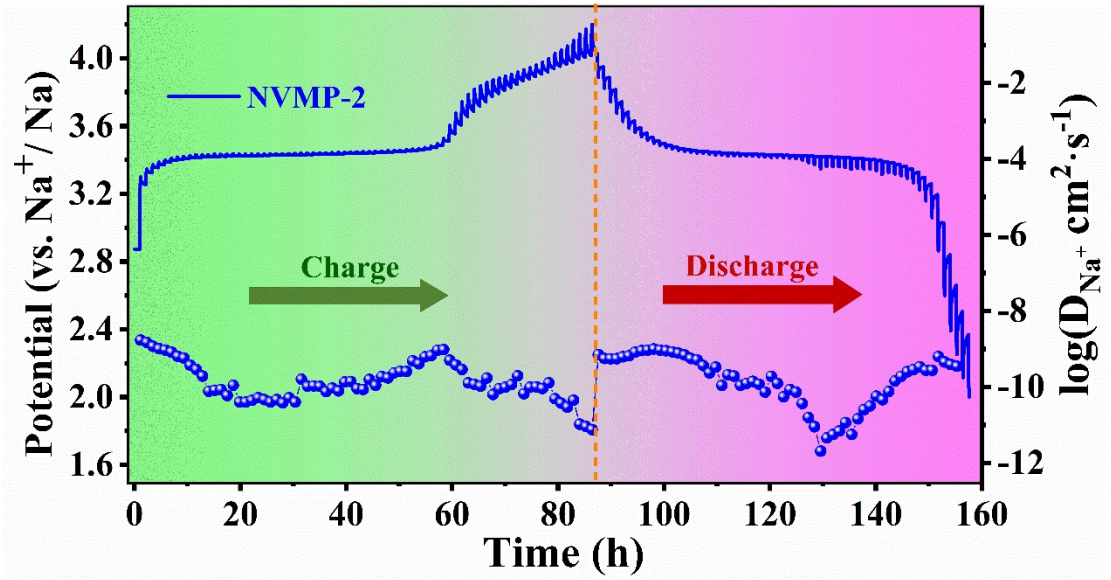

Figure S10. GITT curves and the potential vs *t* profile for the initial charge/discharge of NVMP-2.

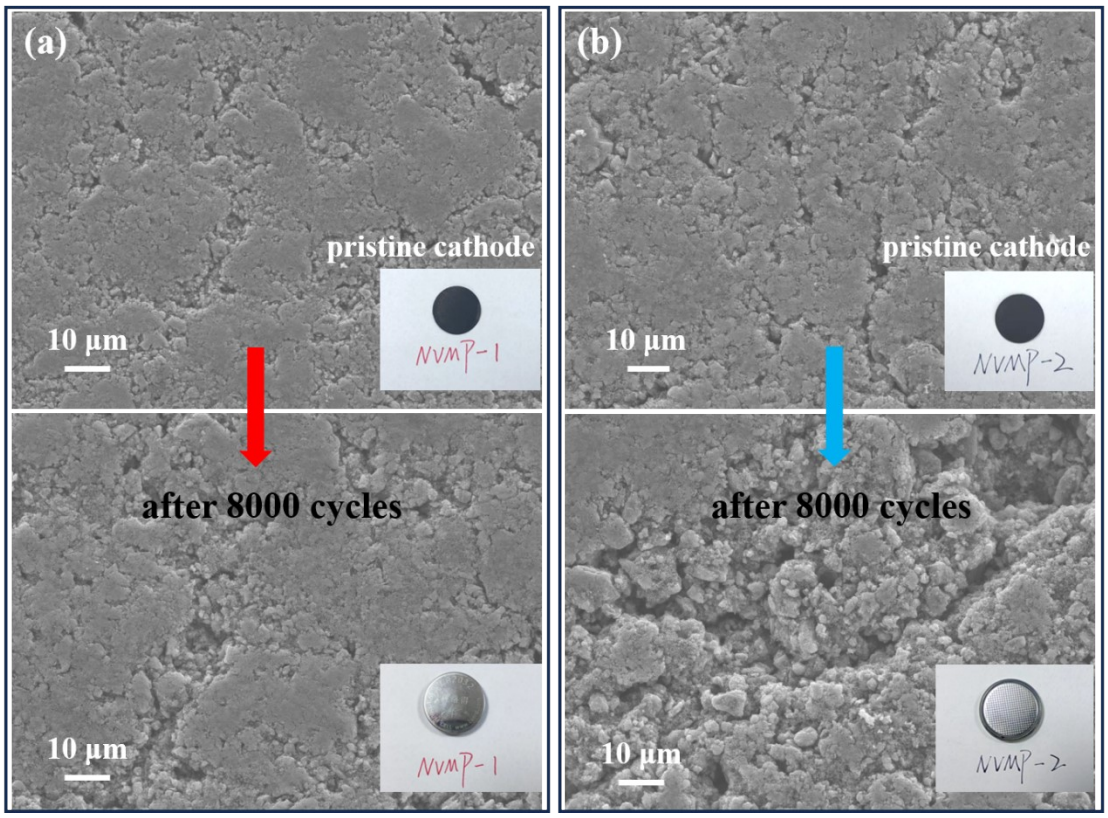

Figure S11. SEM images of pristine and cycled cathode electrodes : (a) NVMP-1 and (b) NVMP-2.

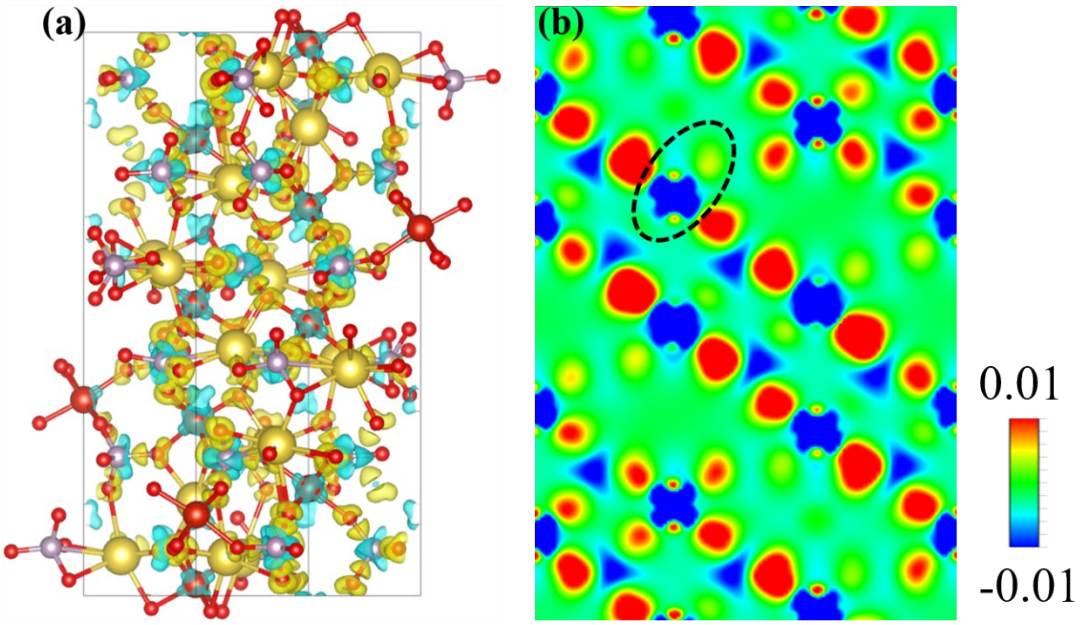

Figure S12. DFT calculation: (a) model and (b) cross-sectional diagrams of charge density difference for $Na_3V_2(PO_4)_3$.

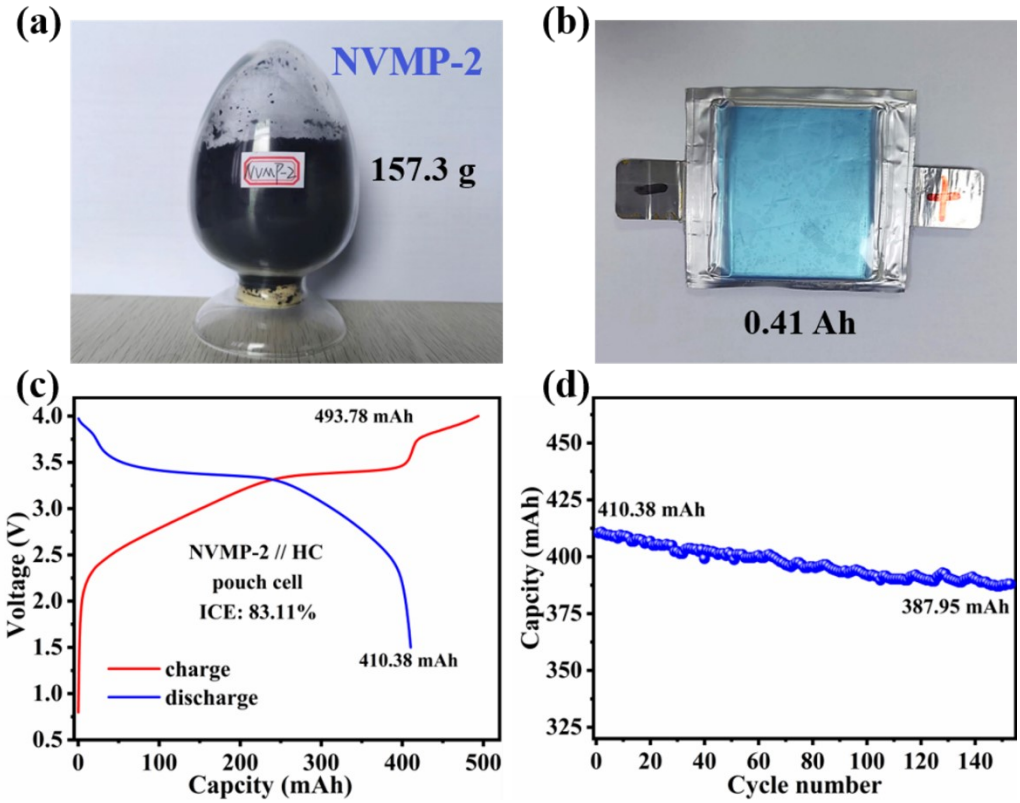

Figure S13. (a) NVMP-2 material and NVMP-2 pouch cell: (b) optical photograph, (c) initial charge/discharge curves, (d) cycling performance.

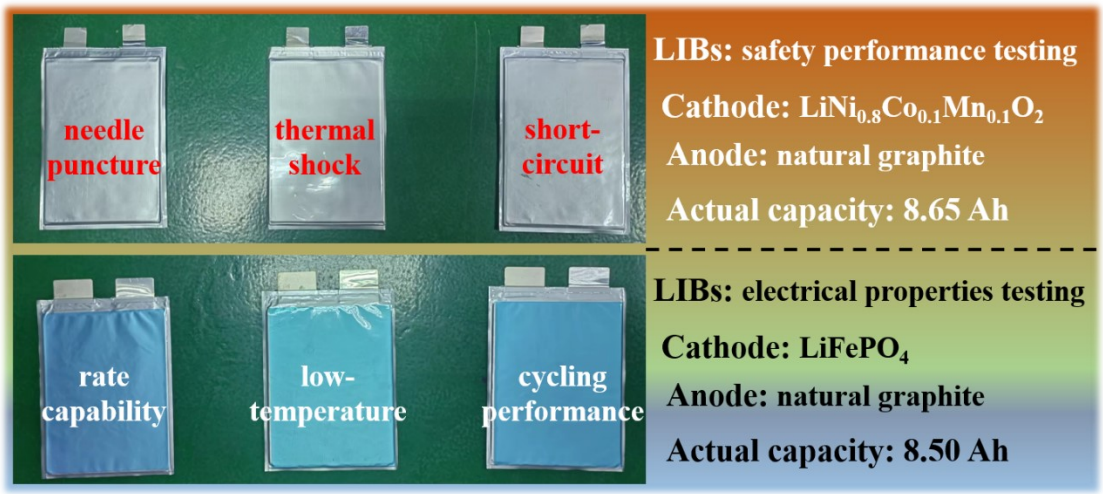

Figure S14. Physical pictures of lithium-ion batteries (LIBs) full-cells used for safety performance and electrical properties testing.

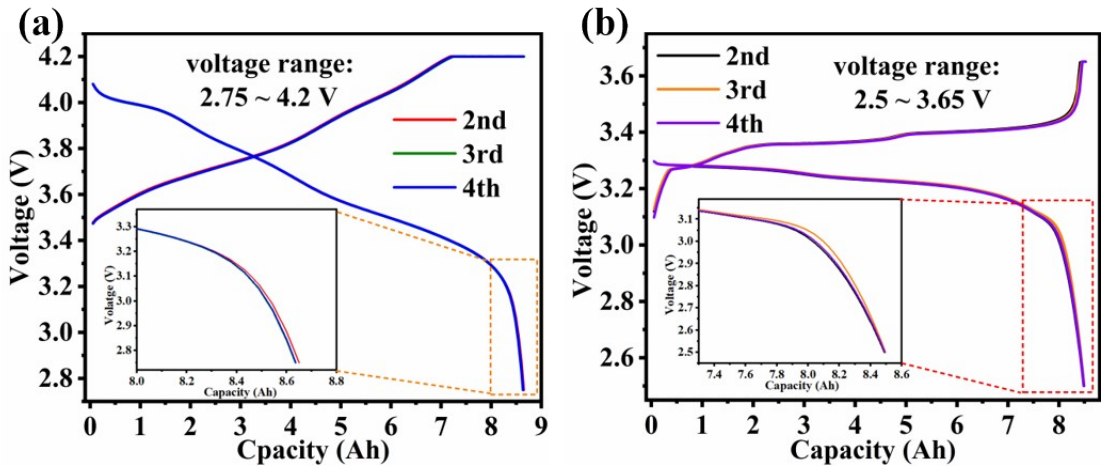

Figure S15. Charge/discharge curves of LIBs full-cells: (a) $LiNi_{0.8}Co_{0.1}Mn_{0.1}O_2$ cathode and (b) $LiFePO_4$ cathode.

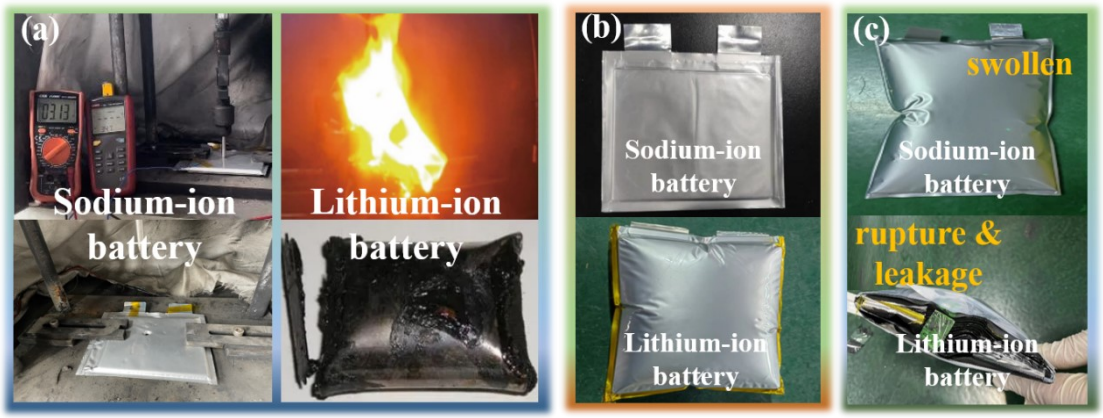

Figure S16. The comparison of safety performance between sodium-ion batteries and lithium-ion batteries: (a) the needle puncture testing, (b) the thermal shock testing; (c) the short-circuit testing.

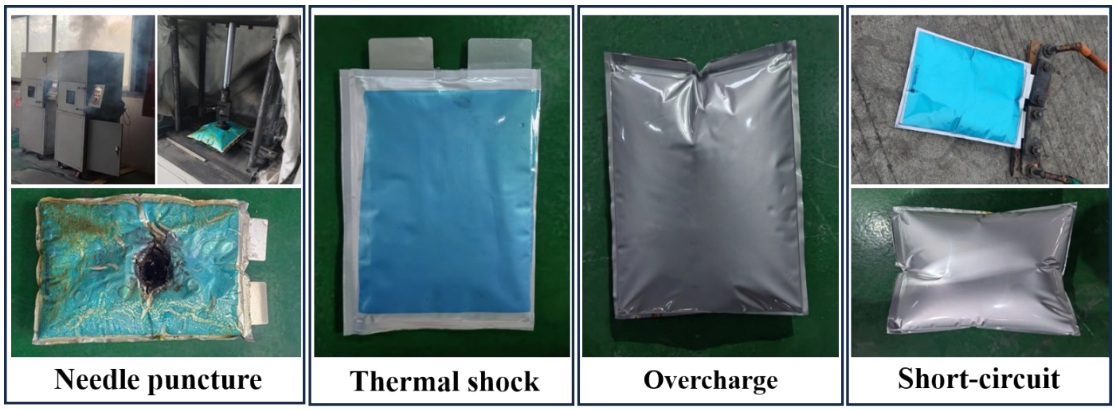

Figure S17. Pictures of $LiFePO_4$ lithium-ion batteries used for safety tests.

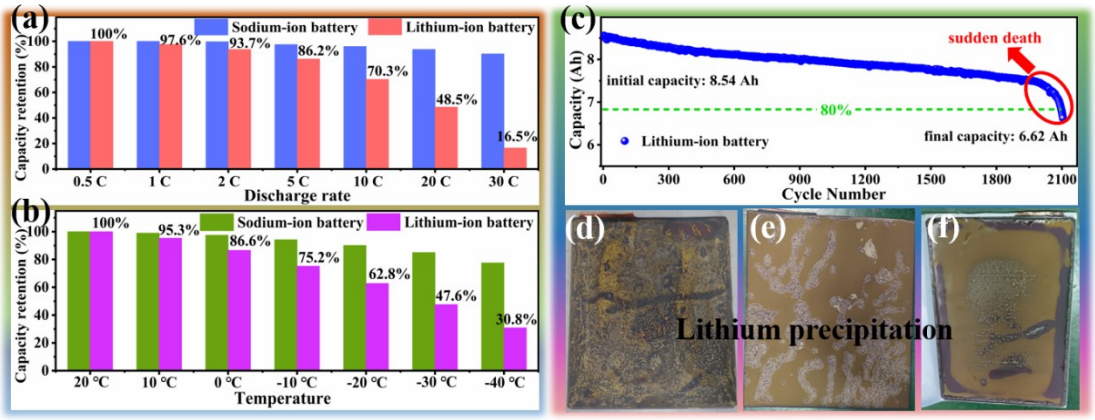

Figure S18. The comparison of electrical performance between sodium-ion batteries and lithium-ion batteries: (a) rate performance; (b) low-temperature performance; (c) cycling performance at 1 C of lithium-ion battery; (d-f) the spent graphite anode electrodes of the lithium-ion batteries that have undergone rate testing, low-temperature testing, and cycling testing.

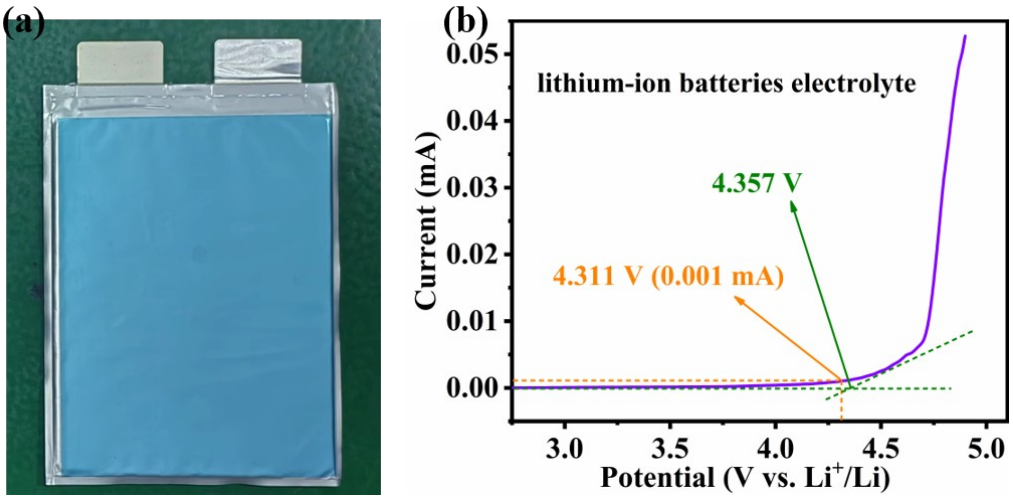

Figure S19. (a) $LiFePO_4$ lithium-ion battery after cycling testing, (b) LSV curve of electrolyte in lithium-ion batteries.

Table S1 The market prices of chemical raw materials in China as of March 2024.

Raw material	Purpose and function	Price ($ per ton)
V_2O_5	vanadium source	19394.9
NH_4VO_3	vanadium source	15238.8
$C_4H_6O_4Mn{\cdot}4H_2O$	manganese source	105.3
$NaH_2PO_4{\cdot}2H_2O$	sodium / phosphorus source	831.2
$Na_2HPO_4{\cdot}2H_2O$	sodium / phosphorus source	858.9
Na_2CO_3	sodium source	554.1
$NH_4H_2PO_4$	phosphorus source	1025.1
glucose/starch	carbon source	387.9
citric acid	carbon source	623.4
CMC	carbon source / thickener	1246.8
PAN / PEO / PVDF	electrospun polymer	2493.6 (PAN)
methyl alcohol	solvent	335.4
deionized water	solvent	27.7
absolute methanol	solvent	415.6
absolute alcohol	solvent	969.7
DMF / DMAc	solvent	1039 (DMF)
polyethylene glycol	solvent / surface active agent	1385.3

Table S2 Comparison of preparation methods for cathode materials.

Methods	References	Solvent (per 100 g product)	Time Consumption	Energy Consumption	Yield Level	Waste gas / Wastewate
Solid-state reaction	1, 2	alcohol (500 mL)	short	low	g	/
Hydrothermal / Solvothermal	3, 4	CH_3OH (2500 mL)	long	high	g	secondary pollution
Sol-gel	5, 6	water (50150 mL)	long	high	g	/
Electrospinning	7, 8	ethanol/methanol/water (more than 2000 mL)	long	normal	g	secondary pollution
Freeze-drying	9	water (10500 mL)	long	high	g	secondary pollution
Spray-drying	10, 11	water (17000 mL)	short	low	kg	/
Suspensoid quick-drying	this work	water (330 mL)	short	low	kg	/

Table S3 The detailed structural information of NVMP-1, NVMP -2 and NVP.

Sample	Reliability factors		Lattice parameters/Å			Occupancy		Na content
	R_{wp}/%	χ^2	a (=b)	c	volume	Na(1) sites	Na(2) sites	-
NVP	9.24	1.66	8.7388	21.8053	1442.8	0.7411	0.7224	2.9021
NVMP-1	9.93	1.29	8.8163	21.6697	1460.7	0.8189	0.7619	3.5057
NVMP-2	9.04	1.20	8.8153	21.7052	1458.6	0.7790	0.7538	3.4782

Table S4 The characteristic parameters of cathode powder materials.

Samples	Particle size / μm			Specific surface area	Tap density	Compacted density	pH
	Dv(10)	Dv(50)	Dv(90)	(m^2 g^{-1})	(g cm^{-3})	(g cm^{-3})	
NVMP-1	3.58	9.84	23.1	27.93	1.02	1.89	7.03
NVMP-2	0.94	6.91	29.2	21.17	0.98	1.61	6.96

Table S5 Comparison of electrolyte retention and energy density of full-cells with different capacities.

	Type	Discharge capacity	Battery weight	Electrolyte dosage	Electrolyte retention	Energy density (entire battery)
1	button full-cell	0.72 mAh	2.88 g	0.082 g	113.9 g Ah^{-1}	0.83 Wh kg^{-1}
2	button full-cell	1.61 mAh	2.90 g	0.079 g	49.1 g Ah^{-1}	1.83 Wh kg^{-1}
3	pouch full-cell	344 mAh	14.05 g	4.23 g	12.3 g Ah^{-1}	80.77 Wh kg^{-1}
4	pouch full-cell	2.1 Ah	65.26 g	19.32 g	9.2 g Ah^{-1}	106.19Wh kg^{-1}
5	pouch full-cell	8.61 Ah	252 g	73.2 g	8.5 g Ah^{-1}	112.75 Wh kg^{-1}

Table S6 Safety tests parameter comparable table.

	Lithium-ion batteries	**Sodium-ion batteries**
Cathode	$LiNi_{0.8}Co_{0.1}Mn_{0.1}O_2$	NVMP-1
Anode	Graphite	Hard carbon
Electrolyte	$LiPF_6$ (1 M) in EC/DEC/FEC = (6:3.5:0.5 vol %)	$NaPF_6$ (1 M) in EC/DEC/FEC = (6:3.5:0.5 vol %)
Needle puncture	Fire breaking out	Normal
Short-circuit	Rupture & leakage	Bulging
Overcharge	Rupture & leakage	Bulging
Thermal shock	Swelling	Normal

Notes and references

1 H. Ding, X. He, Q. Tao, J. Teng, J. Li, Energy Fuels, 2023, **37**, 4132-4142.

2 X. Liu, J. Gong, X. Wei, L. Ni, H. Chen, Q. Zheng, C. Xu, D. Lin, J. Colloid Interf. Sci., 2022, **606**, 1897–1905.

3 S. Sun, Y. Chen, Q. Bai, Z. Tian, Q. Huang, C. Liu, S. He, Y. Yang, Y. Wang, L. Guo, Chem. Eng. J., 2023, **451**, 138780.

4 Y. Qi, J. Zhao, C. Yang, H. Liu, Y.-S. Hu, Small Methods, 2019, **3**, 1800111.

5 J. Li, Y. Chen, S. He, Y. Yang, Y. Wang, L. Guo, Chem. Eng. J., 2023, **452**, 139311.

6 J. Li, Y. Chen, H. Shi, T. Zhou, Z. Tian, Y. Wang, Li Guo, J. Power Sources, 2023, **562**, 232802.

7 L. Liang, X. Li, F. Zhao, J. Zhang, Y. Liu, L. Hou, C. Yuan, Adv. Energy Mater., 2021, **11**, 2100287.

8 L. Yang, W. Wang, M. Hu, J. Shao, R. Lv, J. Energy Chem., 2018, **27**, 1439-1445.

9 E. Gu, S. Liu, Z. Zhang, Y. Fang, X. Zhou, J. Bao, J. Alloys Compd., 2018, **767**, 131-140.

10 G. Cui, Q. Dong, Z. Wang, X.-Z. Liao, S. Yuan, M. Jiang, Y. Shen, H. Wang, H. Che, Y.-S. He, Z.-F. Ma, Nano Energy, 2021, **89**, 106462.

11 C. Shen, H. Long, G. Wang, W. Lu, L. Shao, K. Xie, J. Mater. Chem. A, 2018, **6**, 6007-6014.